

Stimulated Raman backscatter leading to electron acoustic Thomson scatter

David J. Strozzi, Ed A. Williams, A. Bruce Langdon
Lawrence Livermore National Lab (LLNL)
Livermore, CA 94550 USA

Work performed under the auspices of the U.S. Department of Energy by University of California, Lawrence Livermore National Laboratory under Contract W-7405-Eng-48.

UCRL-POST-225366

Poster UP1.00107
48th APS-DPP Meeting
Philadelphia, PA
2 November 2006

Summary: Vlasov simulations of Raman backscatter show:

- Kinetic inflation¹ of simulated Raman backscatter (SRBS), and electron acoustic scatter (EAS) in conditions similar to Trident single hot-spot experiments².
 - Inflation accompanied by beam acoustic modes (BAMs)³, and electron acoustic waves (EAWs) which scatter the laser (EAS).
 - EAWs generated by beating of different BAMs - beam acoustic decay (BAD).
 - laser scatters off resulting EAW fluctuations - electron acoustic Thomson scatter (EATS); differs from stimulated electron acoustic scatter (SEAS, parametric decay of pump).
- SRBS with weak pump: plasmon larger away from laser entrance due to spatial variation in electron distribution, unlike linear convective steady state.
 - Envelope equation gives nonlinear damping and frequency shift for fixed-drive, electrostatic runs that show spatial dependence similar to Morales-O'Neil calculation.
- Runs with Krook operator (to mimic speckle sideloss): inflation sometimes suppressed.
 - Inflation may be suppressed even when trapped electron bounce frequency $\sim 6x$ Krook relaxation rate.
- Broadband seeding in forward and backward light waves has no effect on inflation.
 - EAS level is constant w.r.t. bandwidth, implying EAS is not amplifying the seed.
- Runs in inhomogeneous density profiles: inflation suppressed, directional asymmetry.
 - SRBS stronger when pump propagates to higher, rather than lower, density.

¹H. X. Vu, D. F. DuBois, B. Bezzerides, Phys. Plasmas 9, 1745 (2002)

²D. S. Montgomery, R. J. Focia, H. A. Rose et al., Phys. Rev. Lett. 87, 155001 (2001)

³L. Yin, W. Daughton, B. J. Albright et al., Phys. Plasmas 13, 072701 (2006)

ELVIS code: Eulerian Vlasov solver; model and geometry

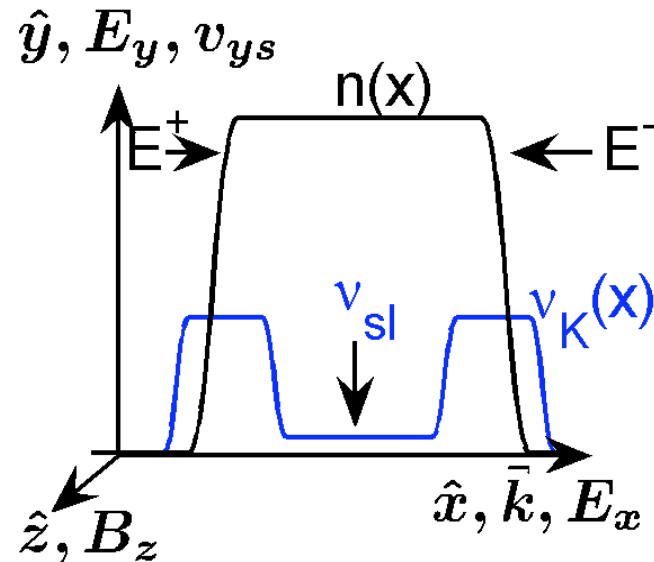
- x kinetic eq.:
$$\left[\partial_t + v_x \partial_x + (Z_s e / m_s) (E_x + v_{ys} B_z) \partial_{v_x} \right] f_s = \nu_{Ks} (x) (n_s \hat{f}_{Ks} - f_s)$$

- Gauss' law:
$$\partial_x E_x = e \epsilon_0^{-1} \sum_s Z_s n_s$$

- Cold, collisionless transverse velocity:
$$m_s \partial_t v_{ys} = e Z_s E_y$$

- Transverse e/m fields: linearly polarized in y:

$$E^\pm \equiv E_y \pm c B_z \quad (\partial_t \pm c \partial_x) E^\pm = -e \epsilon_0^{-1} \sum_s Z_s n_s v_{ys} \quad (E^+, E^-) = (\text{right, left}) \text{ moving}$$



[D. J. Strozzi, M. M. Shoucri, A. Bers, Comp. Phys. Comm. 164/1-3 (2004);
 D. J. Strozzi, E. A. Williams, A. B. Langdon, A. Bers, Phys. Plasmas, submitted (2006)]

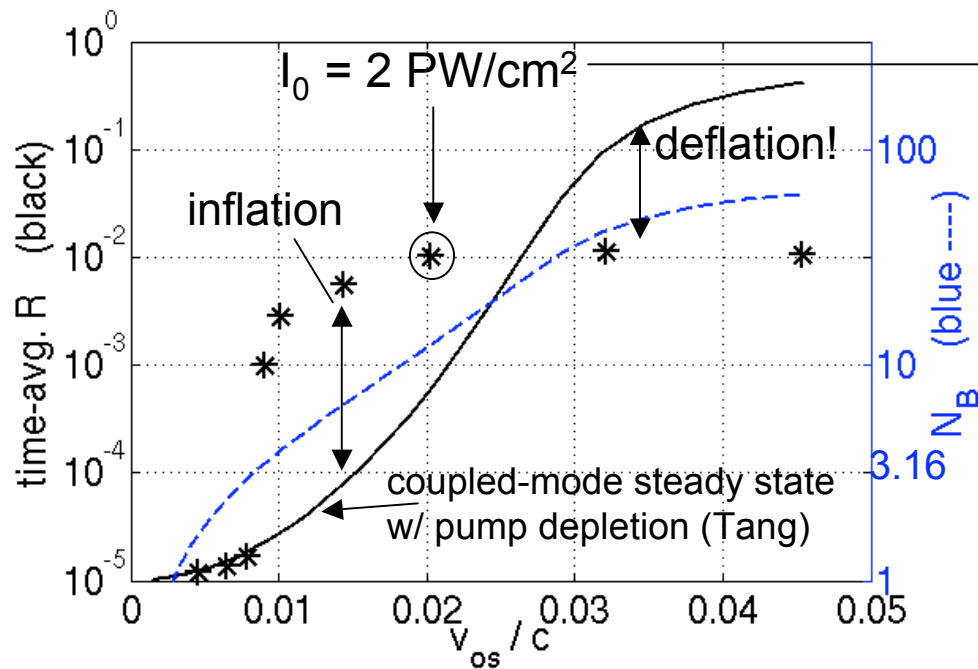
Kinetic inflation occurs for Trident single-hot-spot conditions

- pump: $\lambda_{0v} = 527 \text{ nm}$, $v_{os}/c = (I_0 [\text{PW}/\text{cm}^2] / 4930)^{1/2}$ (vacuum), v_{os}/c (absolute inst.) = 0.078
- plasma: $n_0/n_{cr} = 0.025$ ($\omega_p/\omega_0 = 0.158$), $T_e = 500 \text{ eV}$, fixed ions, $v_{sl} = 0$
- reflected light seed: $I_1 = 10^{-5} I_0$, $\omega_{1s}/\omega_0 = 0.807$, matched EPW: $k_2\lambda_D = 0.352$
- numerics: $dx/\lambda_{0v} = dt \omega_0/(2\pi) = 0.0281$, $dv/v_{Te} = 0.0387$

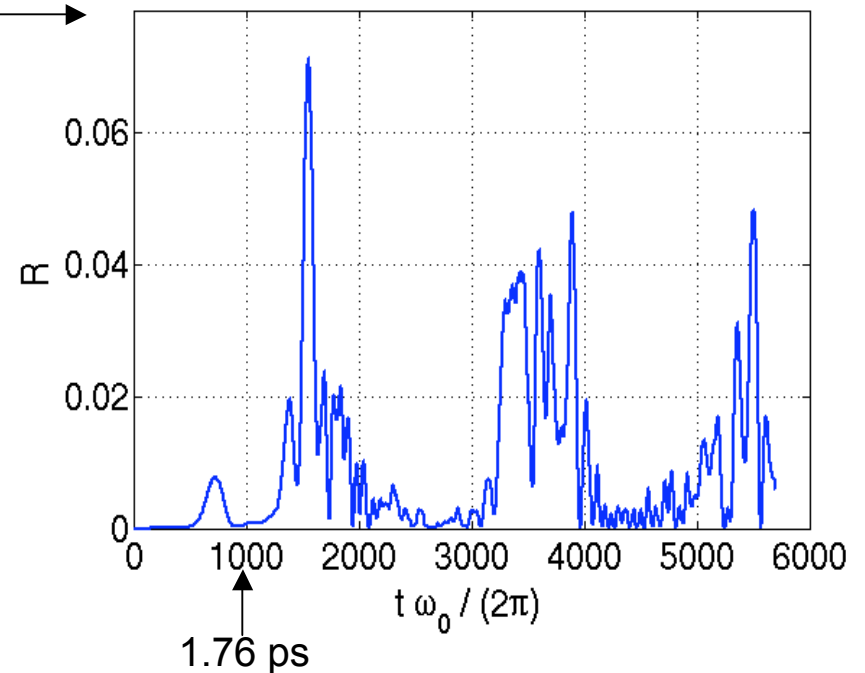
$N_B = \#$ of bounce cycles trapped e^- completes as it crosses plasma; computed in convective steady state. Should be > 1 for trapping to play any role; actually ~ 3 for inflation.

$$N_B = \frac{1}{2\pi} \int_0^L dx k_B \quad k_B = \frac{\omega_B}{v_{ph}} \quad \frac{\omega_B}{\omega_p} = \sqrt{\frac{\delta n}{n_0}}$$

Time-averaged reflectivity (* = runs)

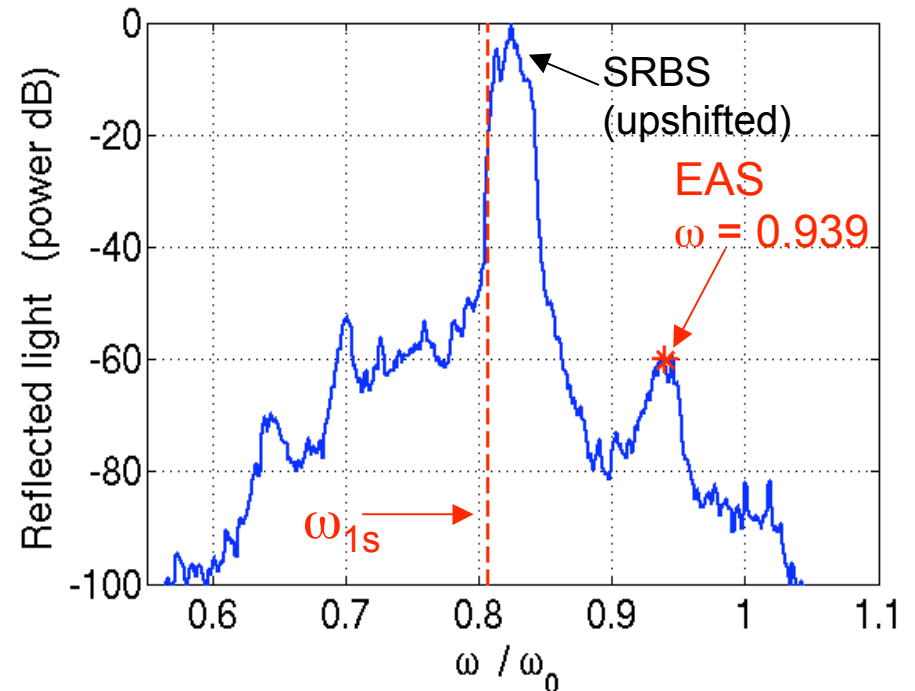
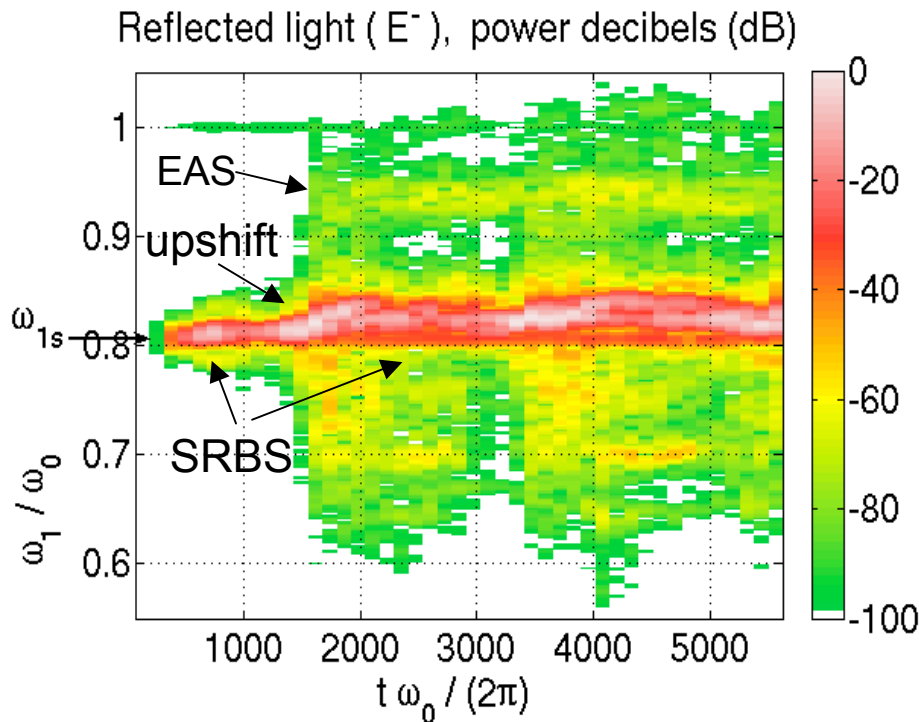


$v_{os}/c = 0.02$: inflated, bursty SRBS



SRBS light upshifted in ω ; electron acoustic scatter (EAS) observed

$$v_{os}/c = 0.02$$



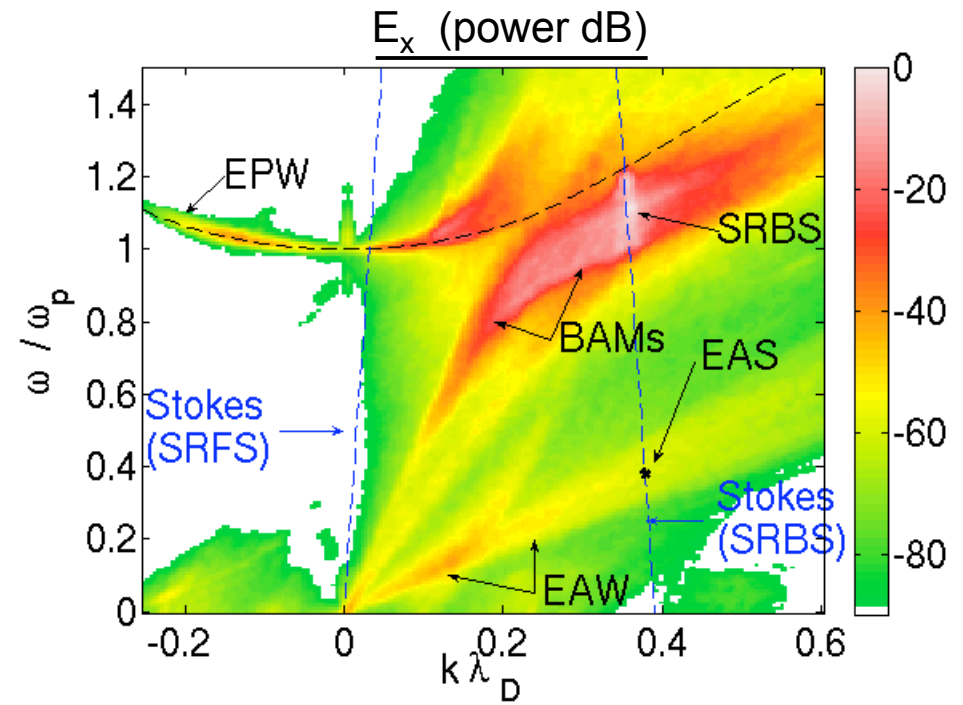
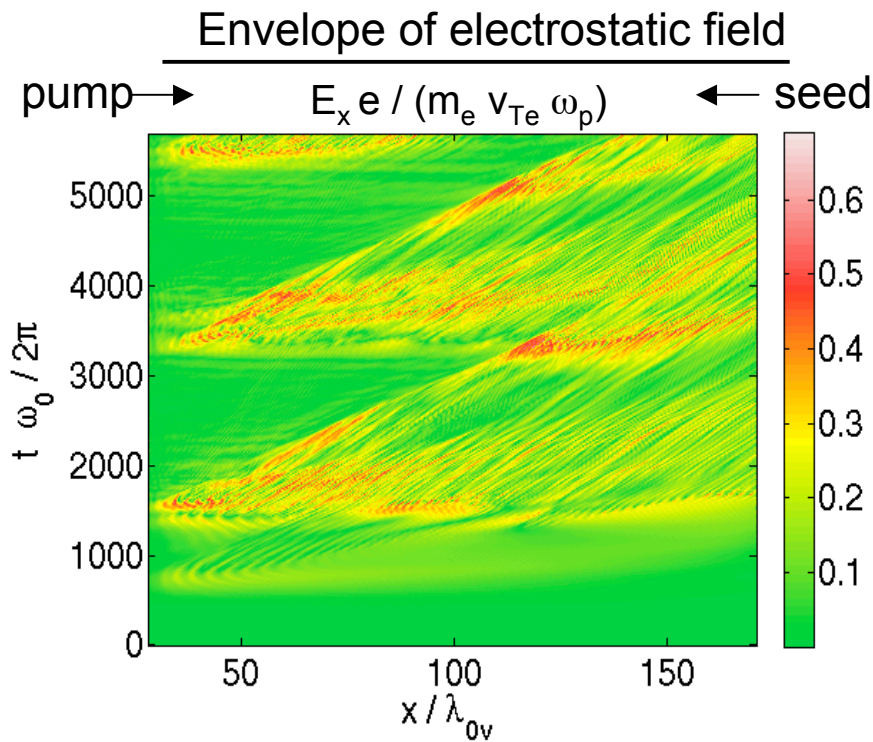
- Trapping of electrons in EPW reduces Landau damping¹, which enhances SRBS reflectivity.
- Trapping also downshifts EPW frequency², which upshifts scattered light frequency.
- EAS light phase-matched with point labeled EAS on next slide; scattering off electron acoustic wave (EAW).

¹T. O'Neil, Phys. Fluids 8, 2255 (1965)

²G. J. Morales and T. M. O'Neil, Phys. Rev. Lett. 28, 417 (1972)

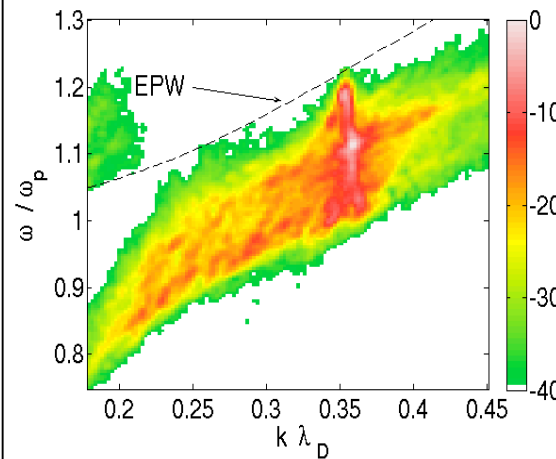
EPW's come in pulses, ω downshifted; beam acoustic modes (BAMs); electron acoustic waves (EAWs)

$$v_{os}/c = 0.02$$

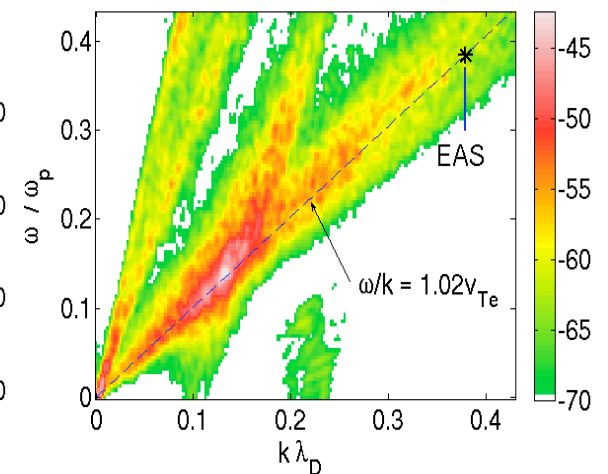


- EPW becomes modulated, streaks move away from pump; some signs of trapped particle instability¹.
 - EAS point phase-matches EAS light on prior slide.
 - EAW is present, but mostly energized well below EAS point, implying it is separately generated.
- ¹S.Brunner, E. J. Valeo, Phys. Rev. Lett. 93, 145003 (2004).

SRBS (zoom)



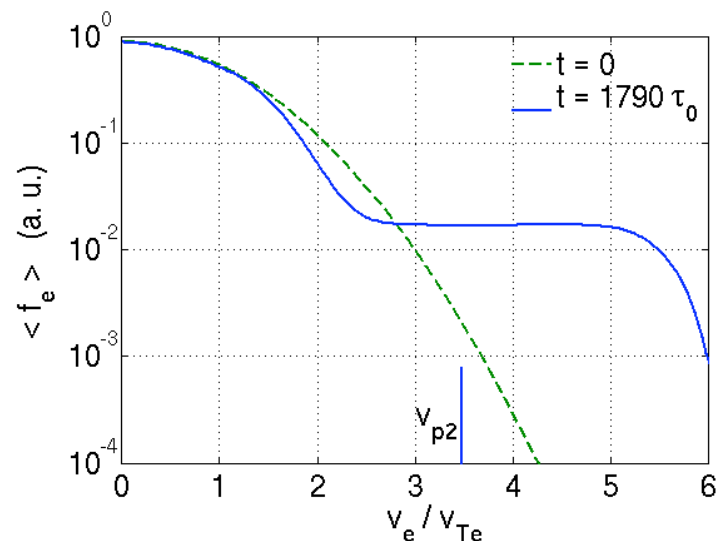
EAW (zoom)



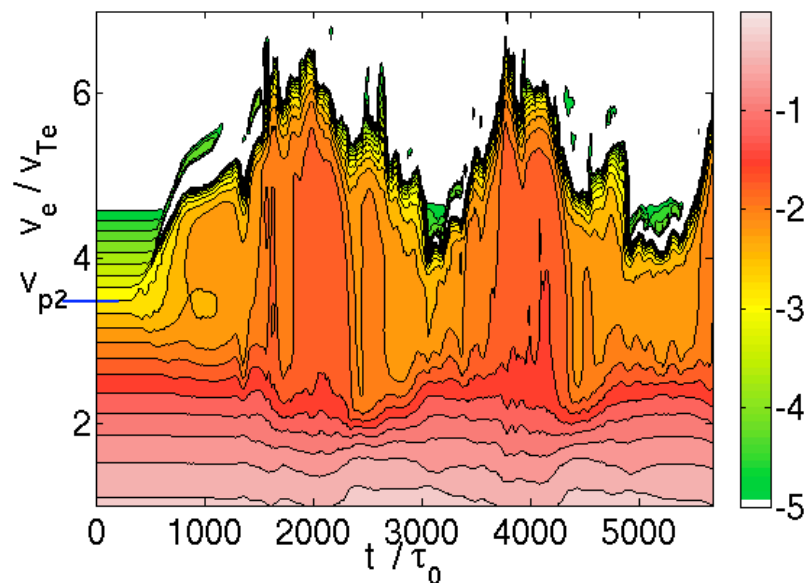
Distribution (f_e) flattened; linear modes of numerical f_e found with Gauss-Hermite projection

$v_{os}/c = 0.02$

f_e avg. over $\Delta t = 1/\omega_p$, $x = [96, 102] \lambda_{0v}$



$\log_{10} \langle f_e \rangle$, a. u.



Linear modes: Gauss-Hermite method; $1 + \chi = 0$

$$f(u) = \sum F_n g_n(u) \quad u = \frac{v - v_0}{\delta v}$$

$$g_n = \frac{1}{\pi^{1/4} \sqrt{2^n n!}} H_n(u) e^{-u^2/2}$$

$$\chi = -(k^2 \delta v)^{-1} \sum F_n \chi_{u,n}(u_p)$$

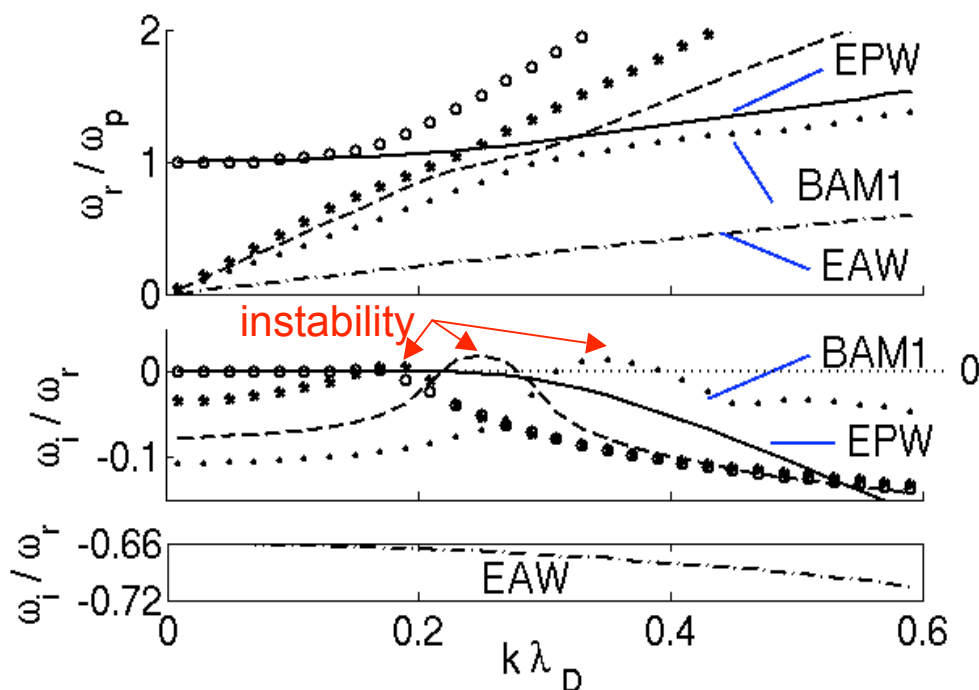
$$\chi_{u,n}(u_p) = \frac{d}{du_p} \int_{-\infty}^{\infty} du \frac{g_n(u)}{u - u_p} = K_{z,n+1}(u_p) Z(u_p/\sqrt{2}) + K_{R,n}(u_p)$$

K's are polynomials; satisfy recurrence relation

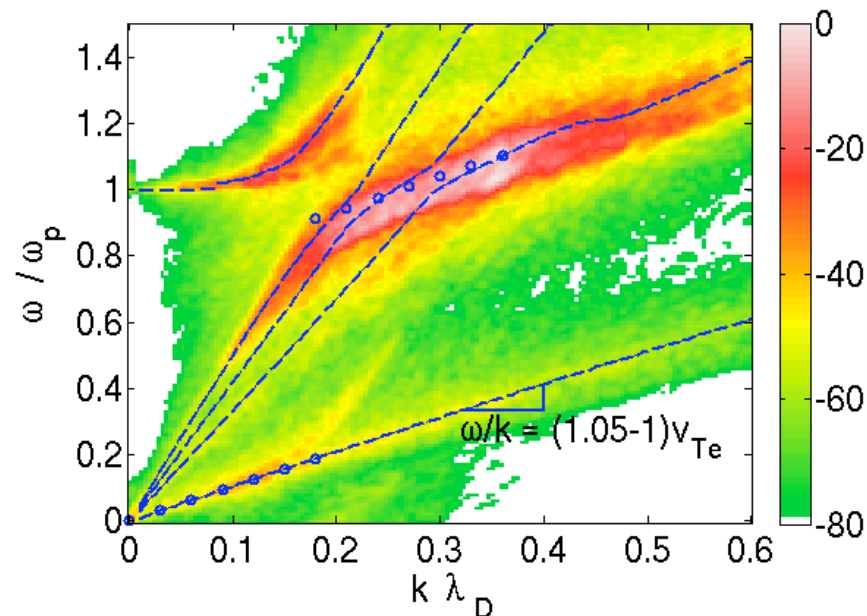
BAMs and EAWs are *linear* modes of modified f_e ; some BAMs are linearly unstable *w/o light-wave coupling*

$$v_{os}/c = 0.02$$

Linear roots found for f_e at $t/\tau_0 = 1790$



E_x , power dB, $t/\tau_0 = 1560 - 2420$



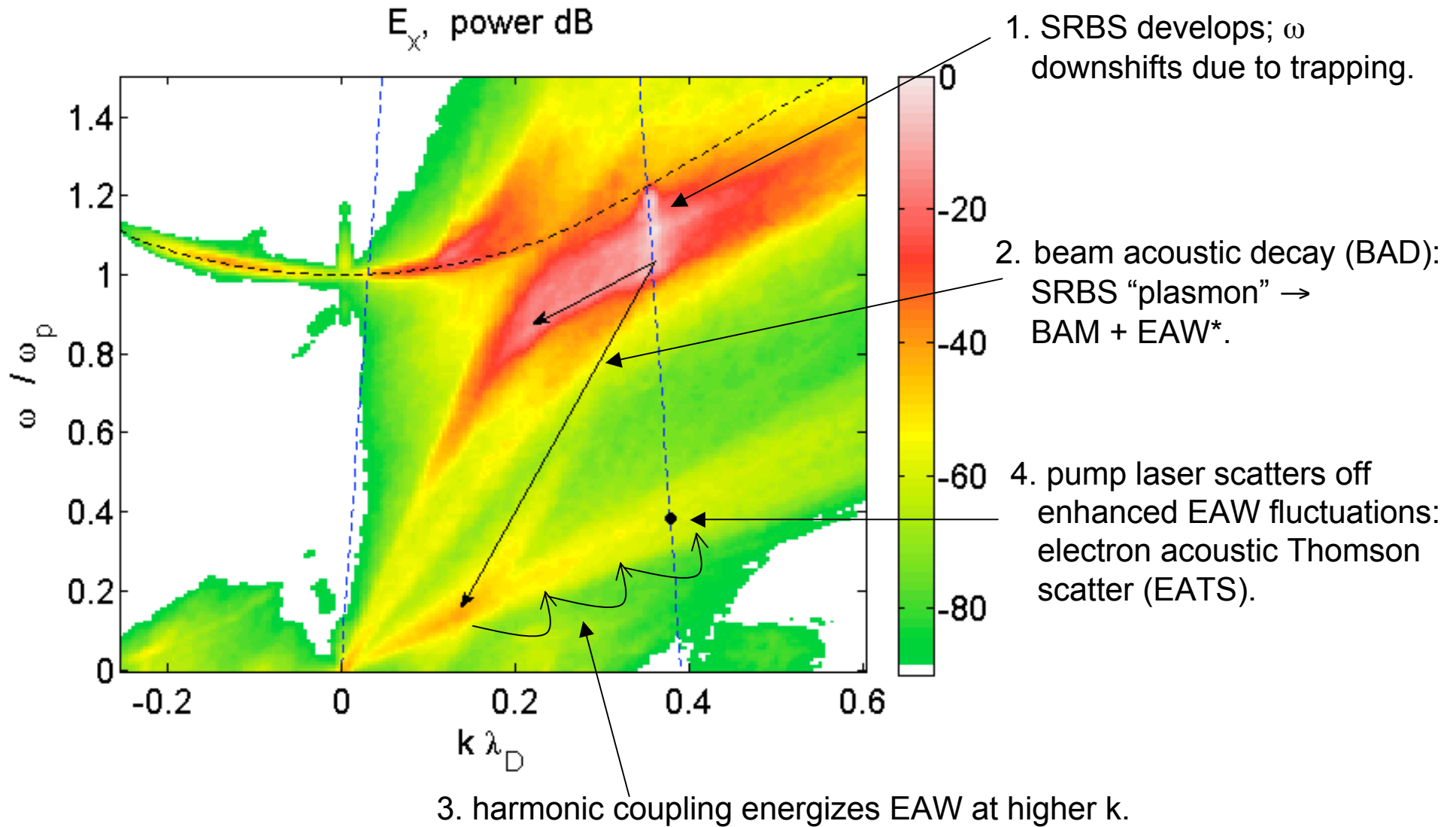
- Blue dashed lines are ω_r from left panel.
- Blue circles are possible BAD daughter modes, with parent BAM chosen near SRBS activity, and EAW daughters on the linear EAW root.

- Linear modes agree well with numerical electrostatic spectrum; EPW for Maxwellian splits into an upper branch and a set of BAMs.
- Some BAMs are linearly unstable, even though no parametric coupling to light waves was included. Indicates beam-plasma instability, related to $df_e/dv > 0$ for some v (Landau growth)
- EAW occurs as a linear mode; heavily damped, no cutoff for high $k\lambda_D$; different from nonlinear, trapping-produced EAW of Rose¹.

¹H. A. Rose and D. A. Russel, Phys. Plasmas 8, 4784 (2001)

Our picture of EAWs and EAS: Beam acoustic decay (BAD) + electron acoustic Thomson scatter (EATS)

$$v_{os}/c = 0.02$$



*Displayed BAD involves an EAW with phase velocity $1.14 v_{Te}$

Bispectral analysis reveals three-wave interactions

x, y, z = real, zero-mean signals; X, Y, Z = their Fourier transforms

• 2-point correlation function:
$$C_2(\tau) = \frac{1}{2T} \int_{-T}^T dt x(t)y(\tau + t)$$

• Power spectrum:
$$P_2(\omega) = \int_{-\infty}^{\infty} d\tau e^{-i\omega\tau} C_2(\tau)$$

Welch's method (J time bins):
$$= \langle P_{2j} \rangle_j \quad P_{2j} = X_j(\omega)Y_j(\omega)$$

• 3-point correlation function:
$$C_3(\tau_1, \tau_2) = \frac{1}{2T} \int_{-T}^T dt x(t)y(\tau_1 + t)z(\tau_2 + t)$$

• Bispectrum (complex, phase info):
$$P_3(\omega_1, \omega_2) = \int_{-\infty}^{\infty} d\tau_1 d\tau_2 e^{-i(\omega_1\tau_1 + \omega_2\tau_2)} C_3(\tau_1, \tau_2)$$

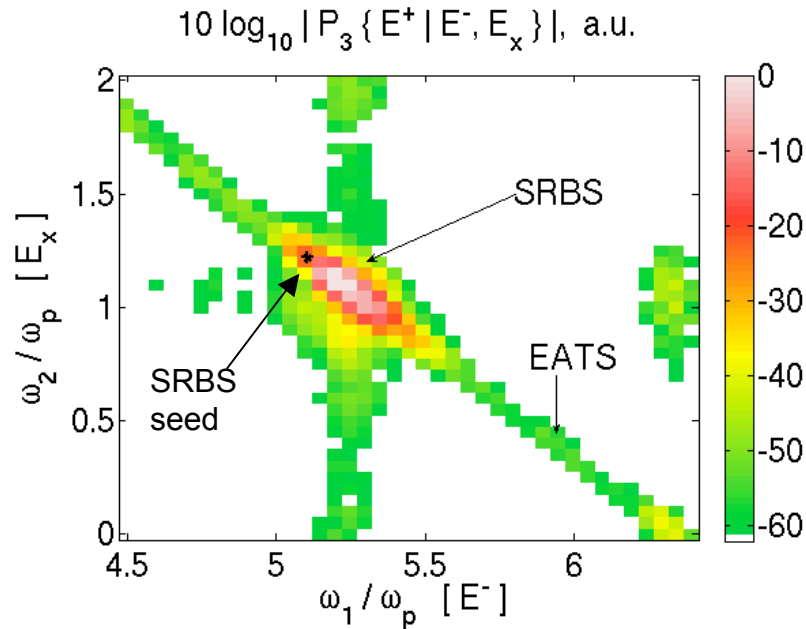
Welch's method:
$$= \langle P_{3j} \rangle_j \quad P_{3j} = X_j(\omega_1 + \omega_2)Y_j(\omega_1)Z_j(\omega_2)$$

• Bicoherence: $0 \leq |b_3| \leq 1$
$$b_3 = \frac{P_3}{\langle |P_{3j}|^2 \rangle_j^{1/2}} = \text{phase-coherent fraction of } P_3$$

The bispectrum shows where the signals satisfy a frequency sum rule; a large bicoherence indicates the signals at these frequencies are in phase (e.g., due to dynamical coupling in a three-wave interaction) and don't match "gratuitously."

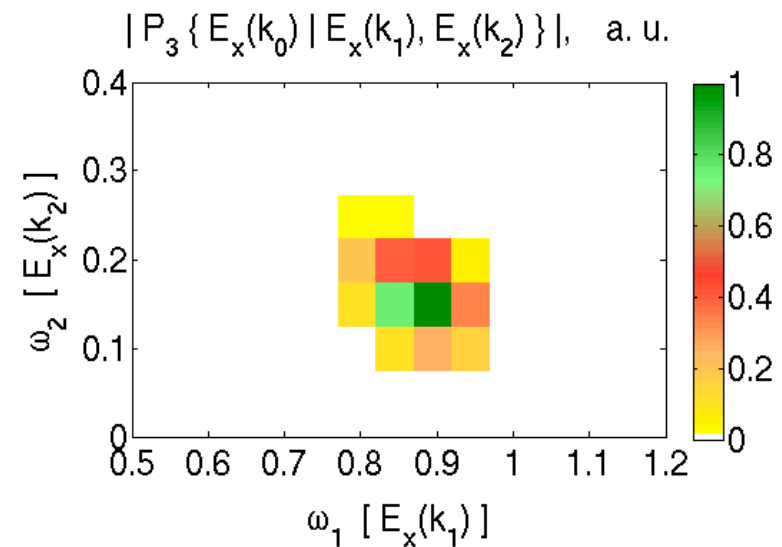
Let $P_3 \{ x | y, z \}$ indicate which fields are used for x, y, z in the prior slide.

$P_3 \{ E^+ | E^-, E_x \}$: shows SRBS, EATS

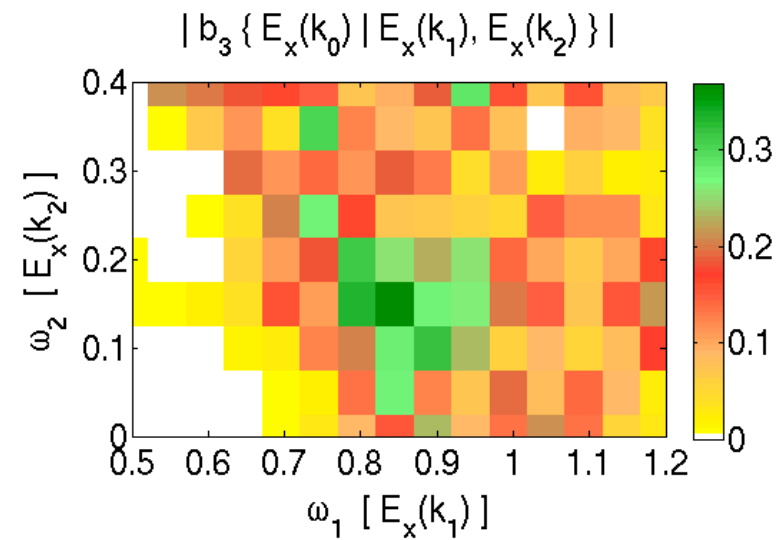
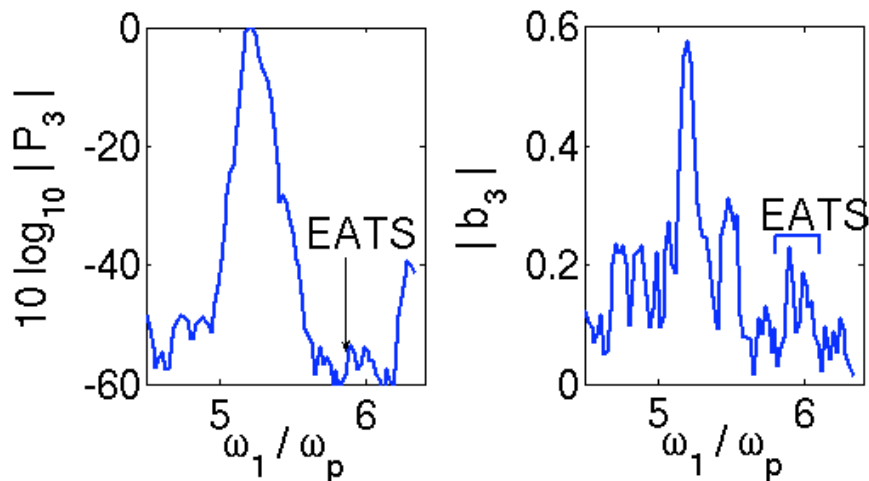


bispectrum of $E_x(k,t)$ for 3 k's
typical for BAD:

$k_i \lambda_D = 0.344, 0.209, 0.136$ for $i = 0, 1, 2$

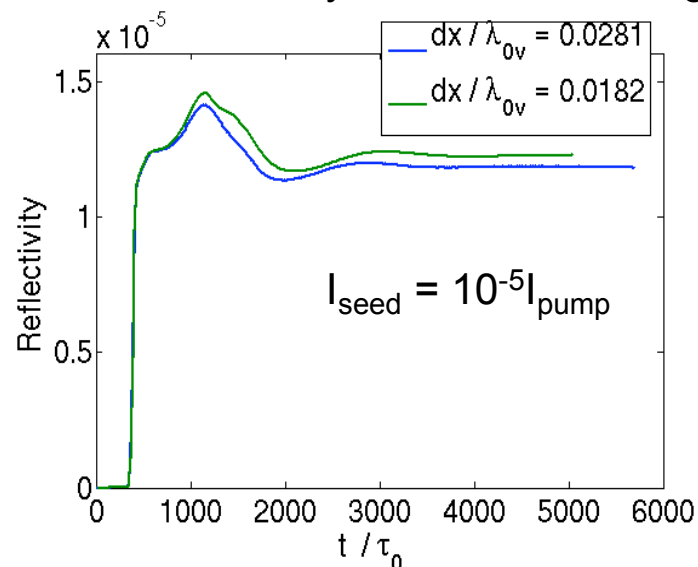


line-outs along $\omega_1 + \omega_2 = \omega_0 =$ pump freq.

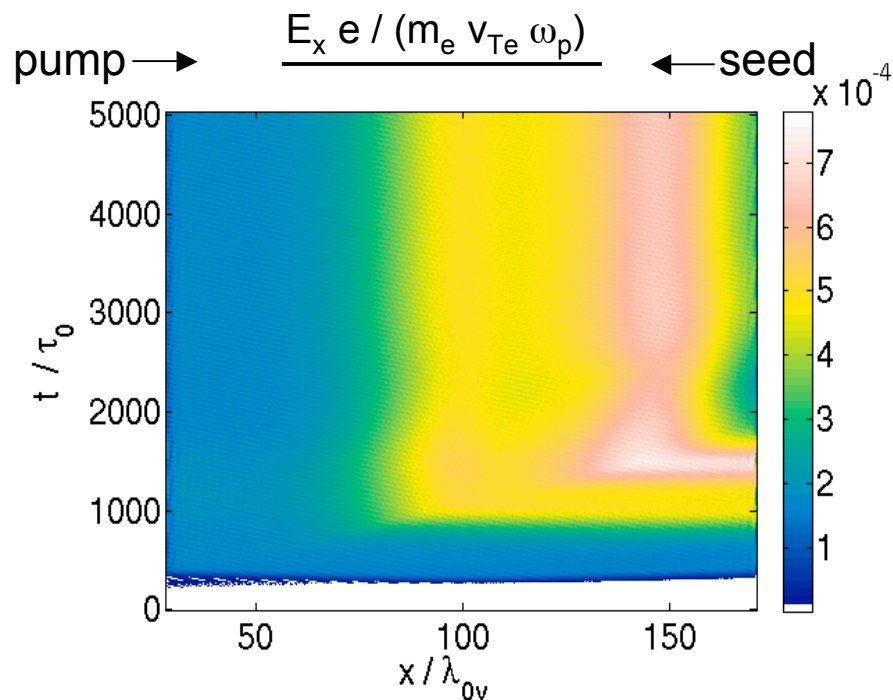


$v_{os}/c = 0.0045$ (weak pump): No inflation; EPW larger *away* from laser entrance!

R becomes steady; numerics converged

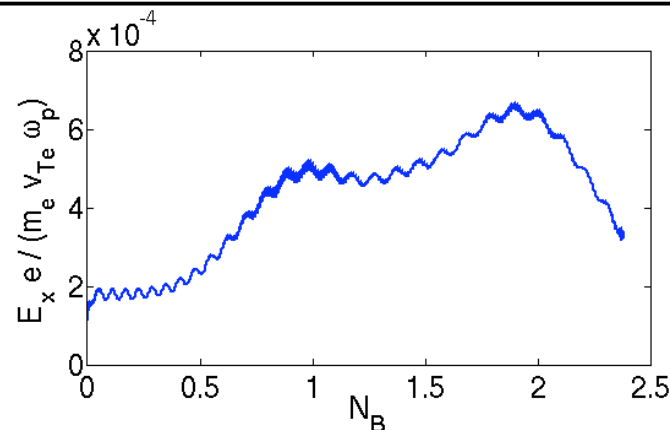


- EPW envelope grows away from pump; in convective steady state we expect growth toward pump, where ponderomotive force is stronger.
- Resonant electrons emerge on the left from clean Maxwellian (due to Krook damping on the edge). As they cross the box they become trapped and bounce. Landau damping and Morales frequency shift, and thus plasma response, vary in space.
- Trapped electrons undergo two full bounces across the box, and yet there is no inflation! O'Neil calculates Landau damping for a free wave to vanish after less than one bounce. Are driven waves different? Is something beyond a damping reduction, somewhere in box, needed for inflation?

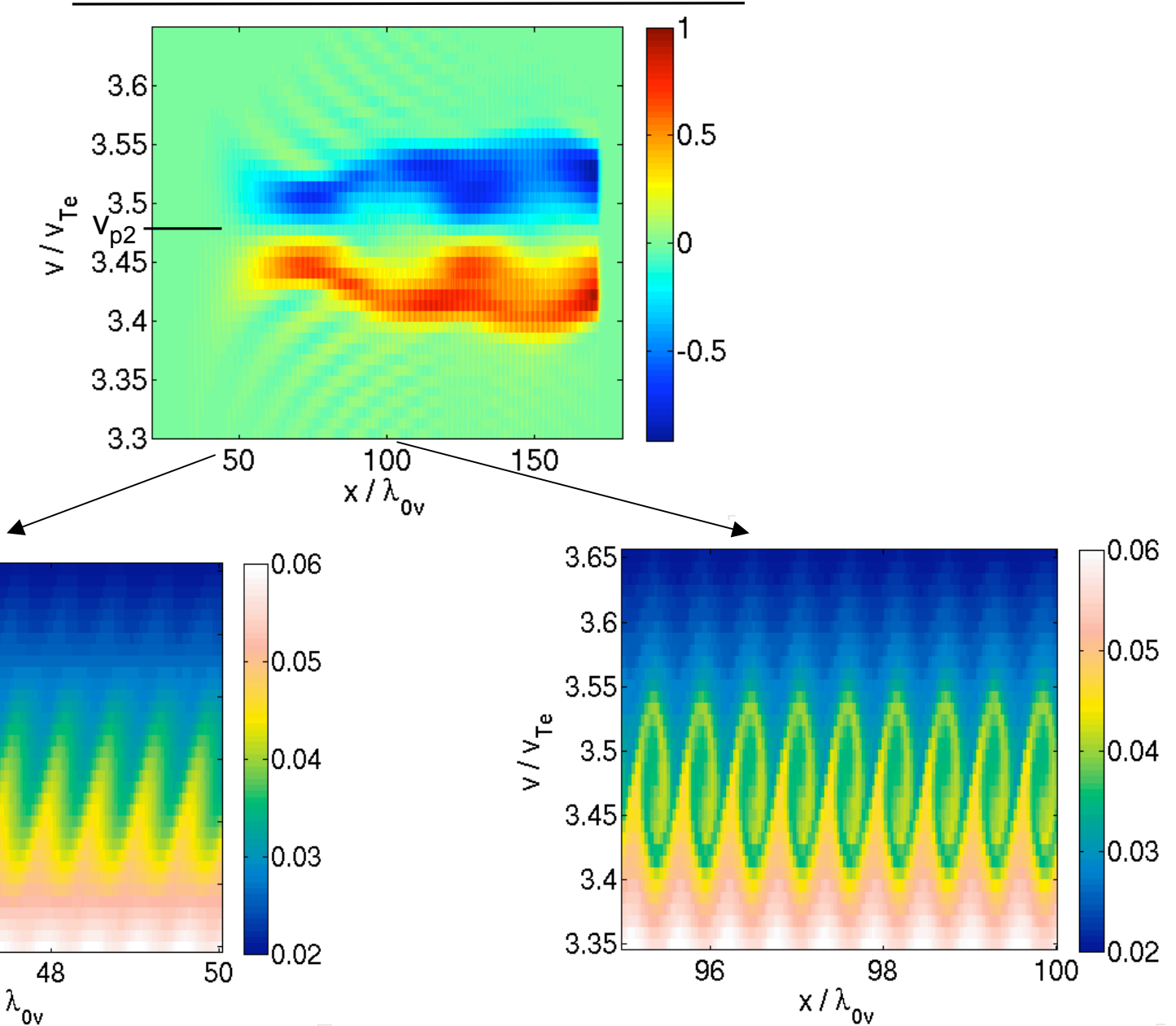


$$N_B(x) = \frac{1}{2\pi} \int_0^x dx' k_B(x')$$

E_x over domain of left panel, $t = 4000\tau_0$



$\delta f = f_e(t=3950\tau_0) - f_e(t=0)$, space-averaged over one EPW wavelength

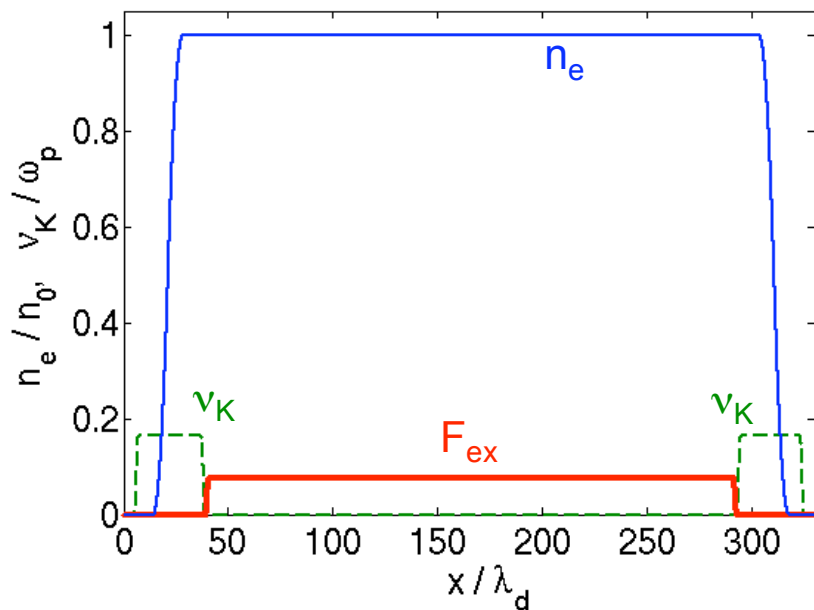


Driven, electrostatic runs: steady state is reached, response varies in x

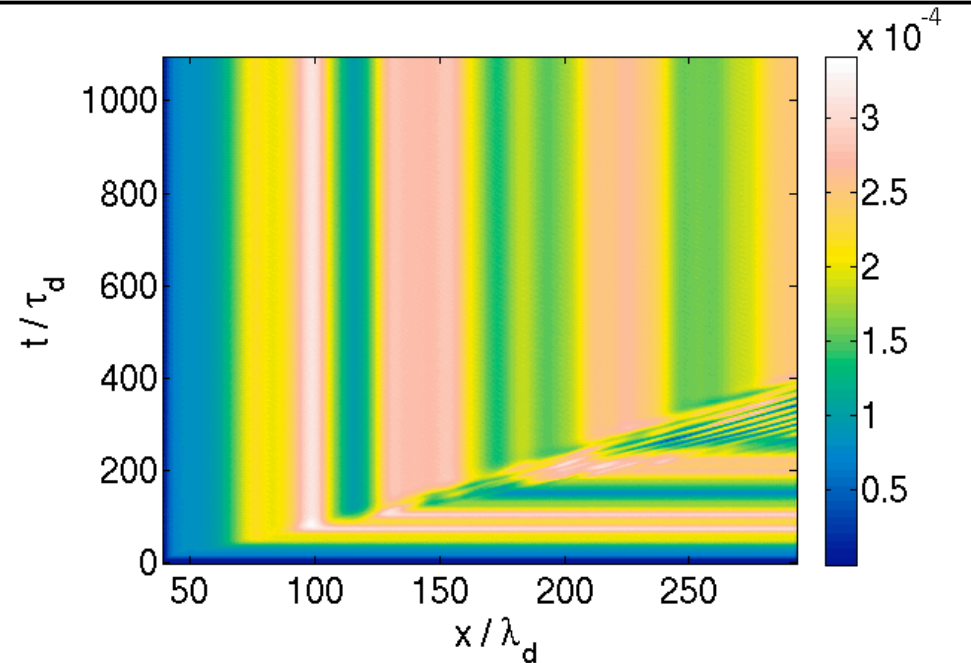
driven e/s

- Plasma parameters: $n_0 = 10^{26} \text{ m}^{-3}$, $\omega_p = 0.564 \text{ rad/fs}$, $T_e = 500 \text{ eV}$
- Drive parameters: $\omega_d / \omega_p = 1.223$, $k_d \lambda_D = 0.352$, $F_{ex} = 1 \rightarrow \delta n_{ex} / n_0 = 5.12\text{E-}6$, force matches ponderomotive force for pump and seed in $v_{os}/c = 0.0045$ Trident run.
- Linear response:
$$\delta n_{in} = -\frac{\chi}{1 + \chi} \delta n_{ex} \rightarrow |\delta n_{in}| = 11.33 |\delta n_{ex}|$$

spatial profiles of n_e , v_K , F_{ex}



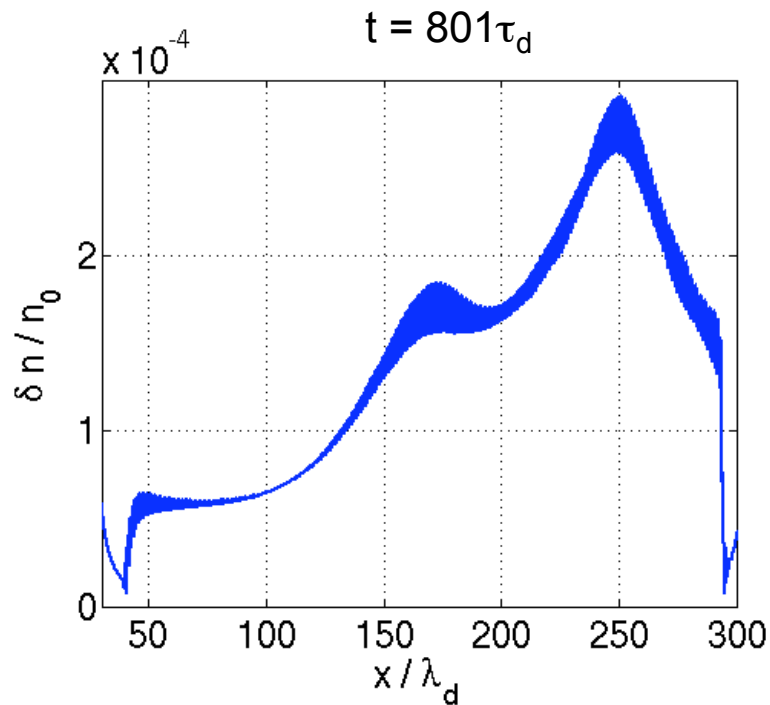
E_x envelope (a.u.) for $F_{ex} = 16$ (strongest drive): steady state reached in this and all runs



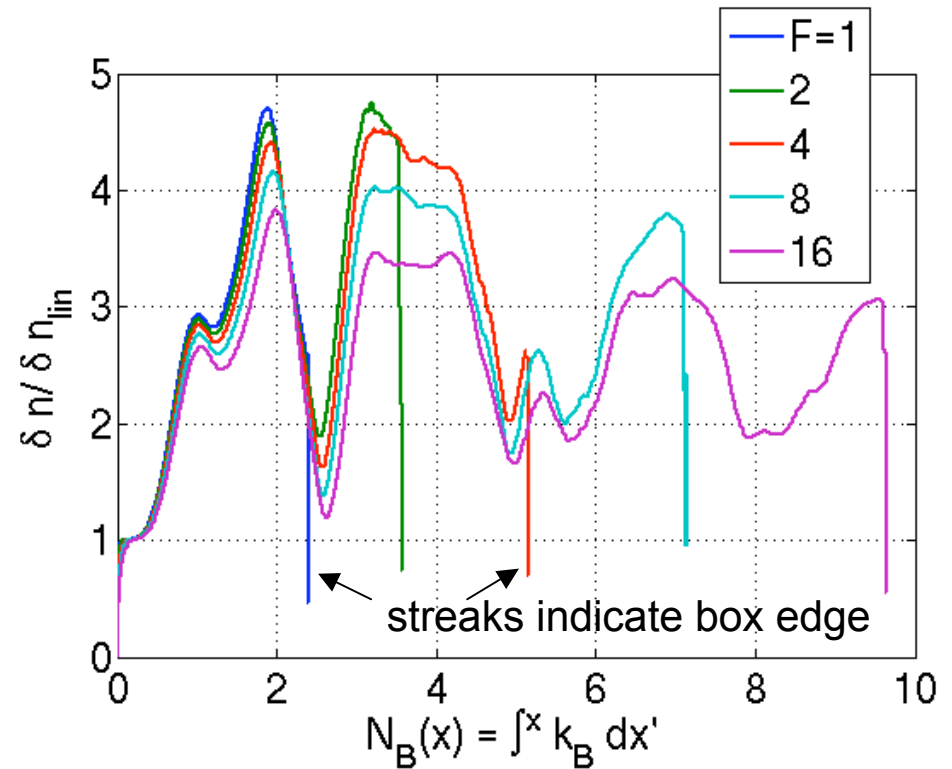
Plasma response for different drive strengths is roughly a universal function of N_B

driven e/s

$F_{\text{ex}} = 1$: weakest drive; steady state profile very similar to $v_{\text{os}}/c = 0.0045$ Trident run



Profiles scaled to linear response are somewhat universal functions, especially for small N_B



Spikes indicate the profile end: more N_B occur in a fixed length for stronger drive.

[B. I. Cohen and A. N. Kaufman, Phys. Fluids **20**, 1113 (1977)]

$$\rho_{X,phys} = \frac{1}{2} \rho_X e^{i(kx - \omega t)} + cc \quad \rho_{in}, \rho_{ex} = \text{external, internal dens. pert.}$$

$$\epsilon(k - i\partial_x, \omega + i\partial_t) \rho_{in} = -\chi \rho_{ex} \quad \epsilon = 1 + \chi$$

$$\epsilon(k - i\partial_x, \omega + i\partial_t) \approx \epsilon_l + \delta\epsilon - i\partial_k \epsilon_{lr} \partial_x + i\partial_\omega \epsilon_{lr} \partial_t$$

$$\chi_l, \epsilon_l = \text{linear response functions} \quad \delta\epsilon = \text{nonlinear component}$$

Steady state: $\partial / \partial t = 0$

$$[\partial_x + \sigma - i(\Delta k_l + \delta k)] \rho_{in} = -i \frac{\chi_l}{\partial_k \epsilon_{lr}} \rho_{ex}$$

This ODE is used to numerically compute σ , δk given the spatial profiles from a run.

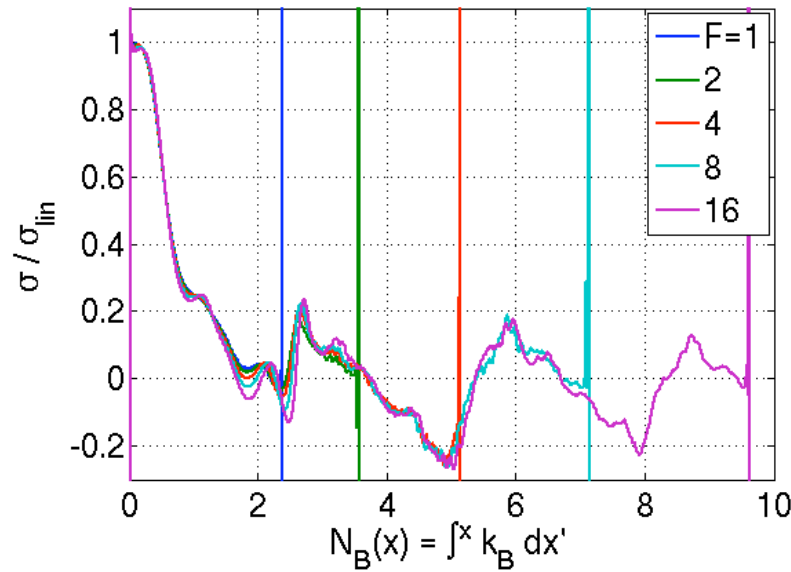
$$\begin{aligned} \sigma &\equiv -\frac{\epsilon_{li} + \delta\epsilon_i}{\partial_k \epsilon_{lr}} = \text{total spatial damping rate} \\ \Delta k_l &\equiv -\frac{\epsilon_{lr}}{\partial_k \epsilon_{lr}} = \text{linear k detuning} \\ \delta k &\equiv -\frac{\delta\epsilon_r}{\partial_k \epsilon_{lr}} = \text{nonlinear k shift} \end{aligned}$$

Inferred damping and k shift from envelope ODE qualitatively resemble Morales-O'Neil calculation

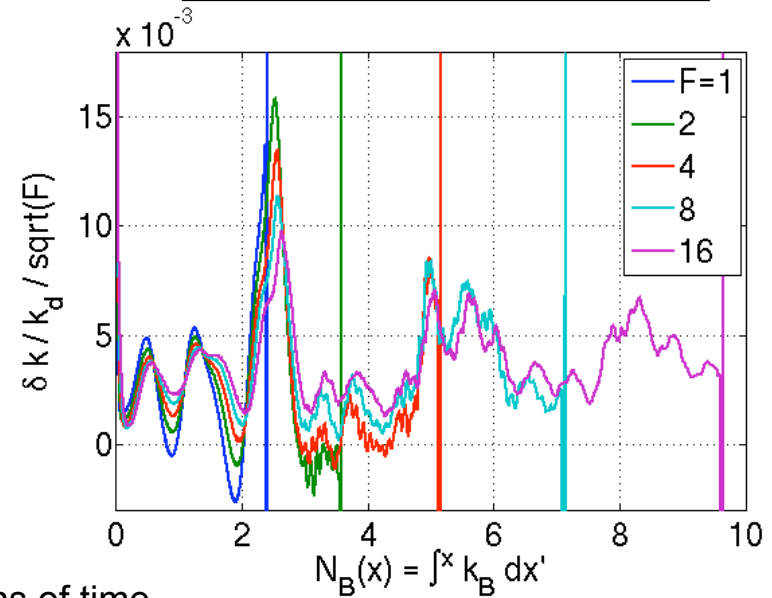
driven e/s

Spikes indicate the profile end: more N_B occur in a fixed length for stronger drive.

Spatial damping rate



k shift; $1/F^{1/2}$ factor accounts for $k_B \sim (\delta n/n_0)^{1/2}$ scaling



Morales-O'Neil solve for damping and freq. shift as functions of time [G. J. Morales and T. M. O'Neil, Phys. Rev. Lett. **28**, 417 (1972)]

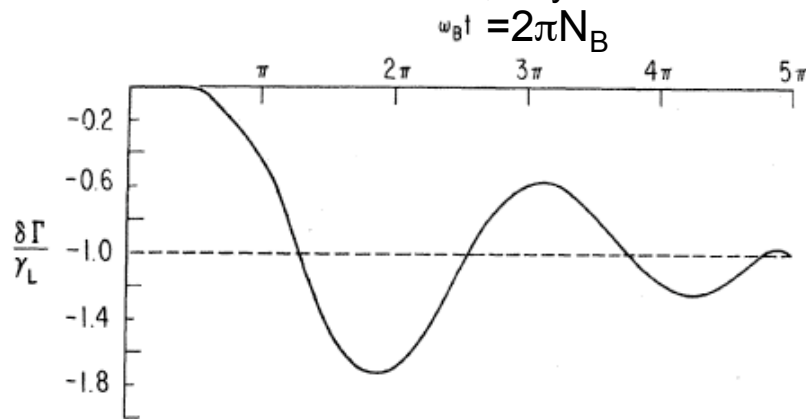


FIG. 1. Damping coefficient shift versus time.

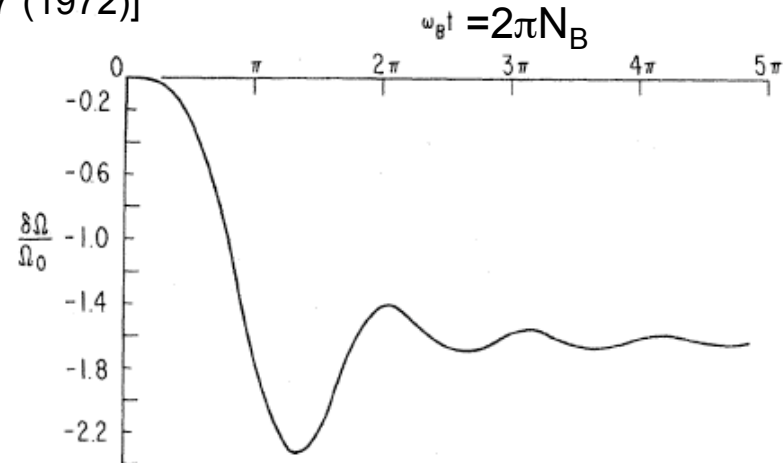


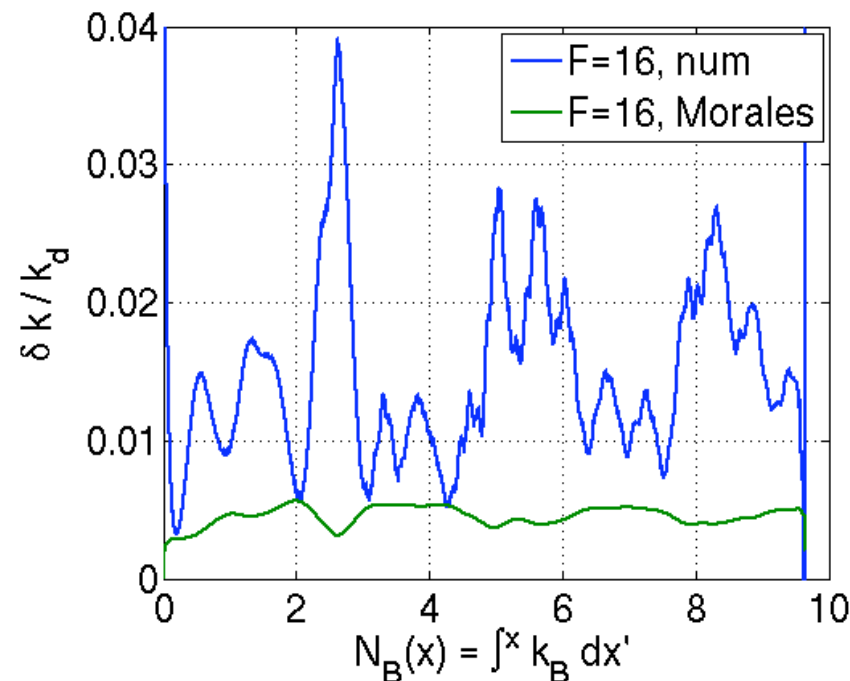
FIG. 2. Frequency shift versus time.

After many bounces:

$$(1) \quad \frac{\delta k}{k_B} = -\alpha \left(\frac{\omega_p}{k} \right)^3 \frac{\omega}{\omega_p} \frac{f_0''}{k \partial \epsilon / \partial k} \quad \alpha = 1.63 \text{ (Morales), } 1.089 \text{ (Dewar adiabatic), } 1.76 \text{ (Rose), and so on}$$

For Maxwellian f_0 :

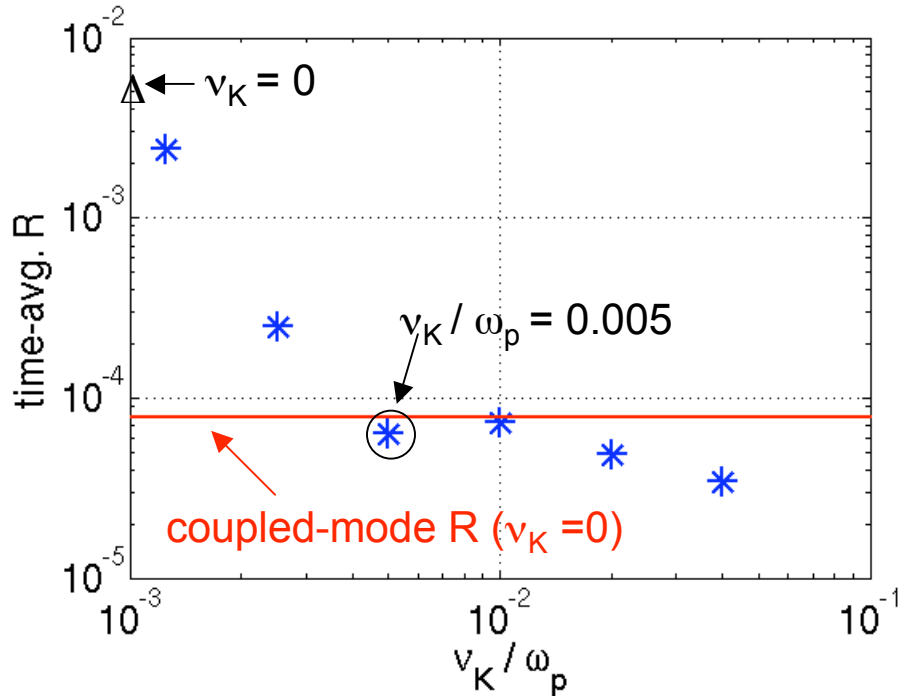
$$\frac{\delta k}{k_B} = -\frac{\alpha}{\sqrt{\pi}} \zeta (2\zeta^2 - 1) \frac{e^{-\zeta^2}}{Z' + (1/2)\zeta Z''} \quad \zeta = \frac{\omega}{k v_{Te} \sqrt{2}} ; k(\omega) \text{ for natural mode}$$



- numerical δk from envelope ODE
- Morales δk from (1) using $\alpha=1.63$ and instantaneous $k_B \sim \delta n^{1/2}$

$v_{os}/c = 0.0142$
 $k_{epw} \lambda_{De} = 0.352$
 $v_{Landau} / \omega_p = 0.0354$

v_K in box center (mimics, e.g., speckle sideloss)

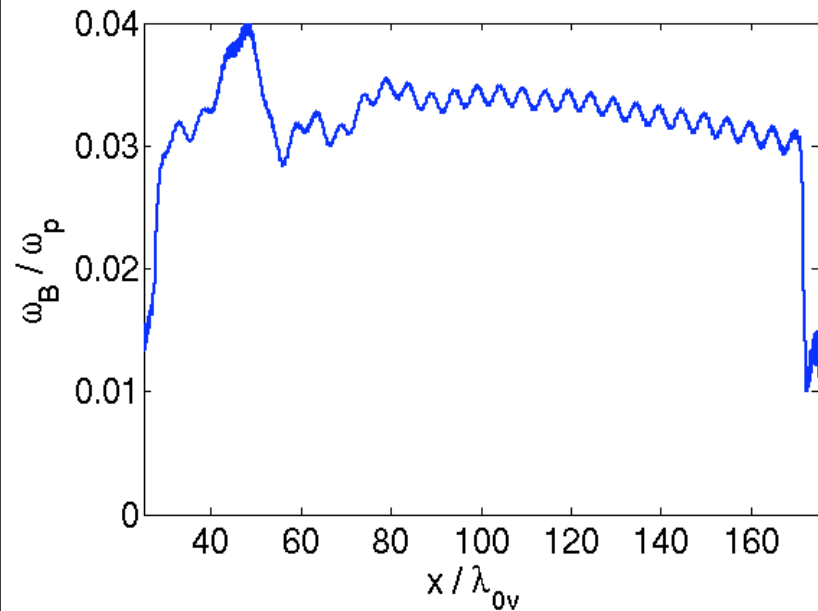


For an f/8 speckle, the sideloss escape rate $v_{sl} = v_{Te} / L_{perp}$ with $L_{perp} = F\lambda_0$ is $v_{sl}/\omega_p = 0.0039$. So sideloss may significantly reduce inflation.

$v_K / \omega_p = 0.005$

$\omega_B \sim 6v_K$, yet no inflation. The ‘lifetime’ of a resonant e- = $1/v_K$, while the bounce period is $2\pi/\omega_B$. So substantial relaxation happens before a complete bounce period.

$\omega_B > 5v_K$ to overcome Krook has been found theoretically; see H. A. Rose, 36th Anomalous Absorption Meeting, 2006.



In prior slides, backscatter seed is monochromatic. Now, add bandwidth to seed, and add seed w/ same spectrum to forward direction (*not* implemented as bandwidth on pump).

Langevin, or Brownian motion, phase generator (A. B. Langdon):

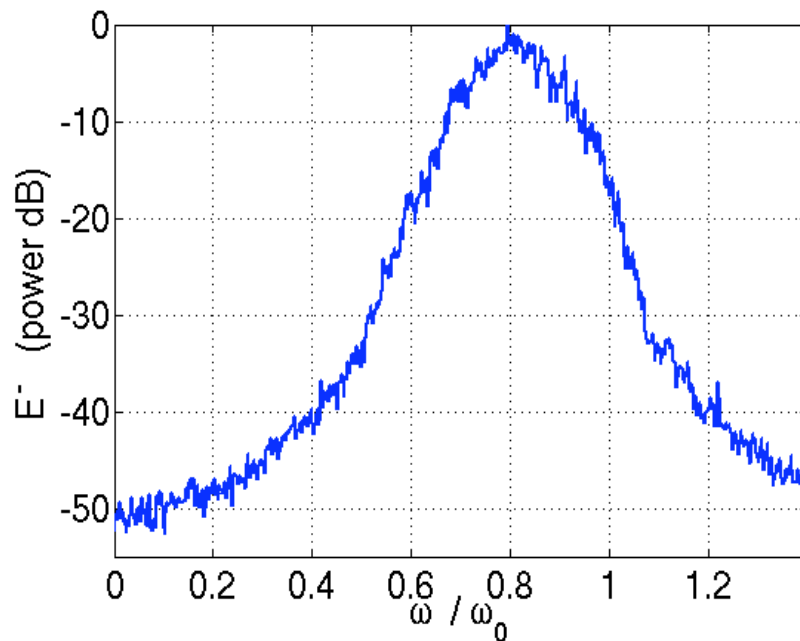
$$E(x_0, t) = E_0 \cos[\omega_0 t + \phi(t)]$$

$$(\phi_{n+1} - \phi_n) - e^{-1/N}(\phi_n - \phi_{n-1}) = \Delta\omega\Delta t\sqrt{2N}(1 - e^{-1/N})r_n$$

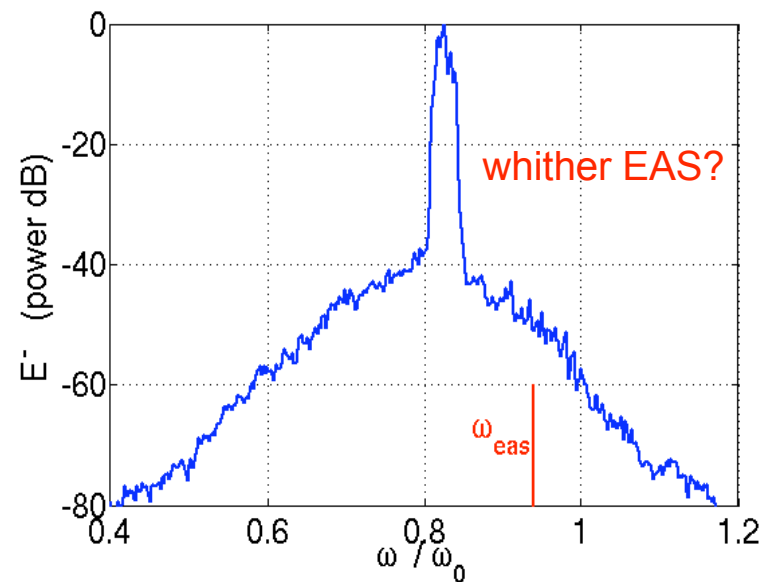
$$P(r_n) = (2\pi)^{-1/2}e^{-r_n^2/2}; \quad r_n = \text{Gaussian random variable}$$

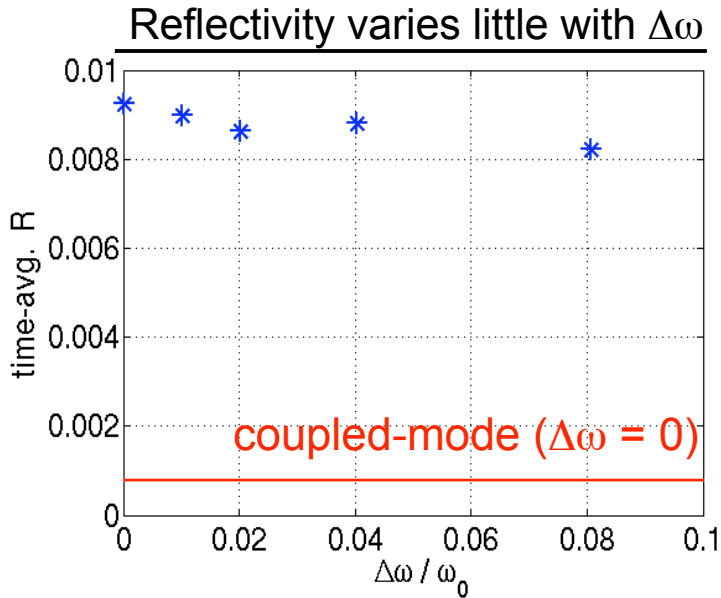
$\Delta\omega$ = bandwidth; Δt = time step; $N \Delta t$ = phase decay time \propto correlation time of $d\phi/dt$

backward seed light wave, $\Delta\omega/\omega_0=0.0806$



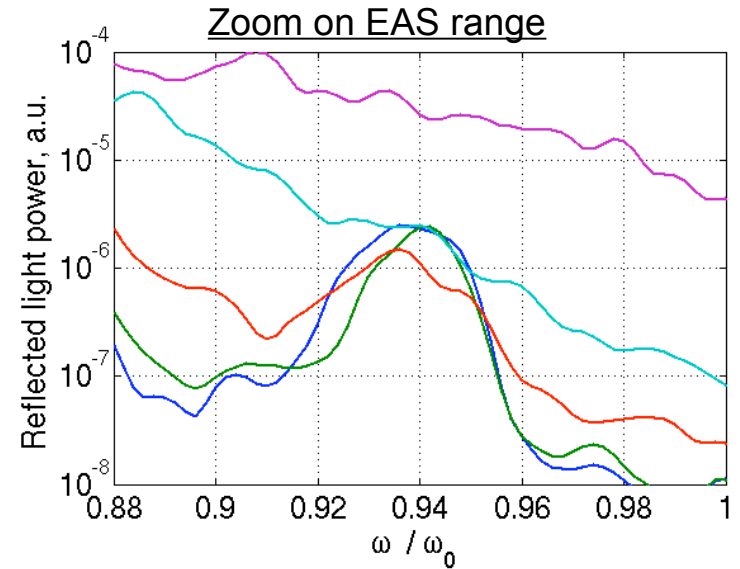
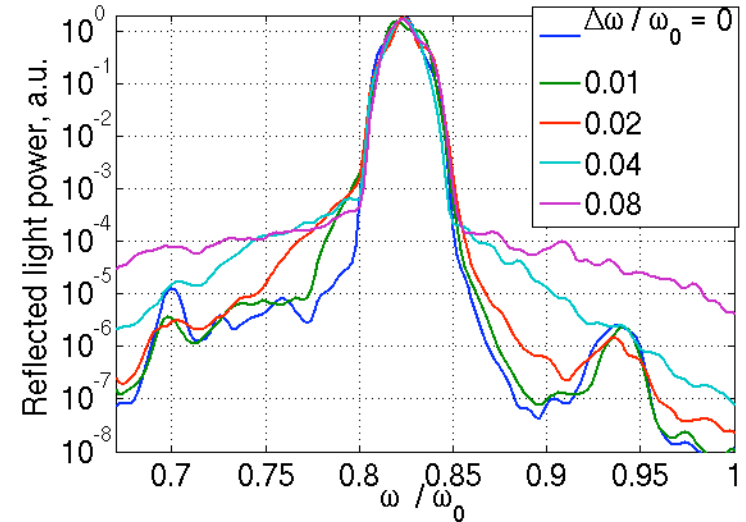
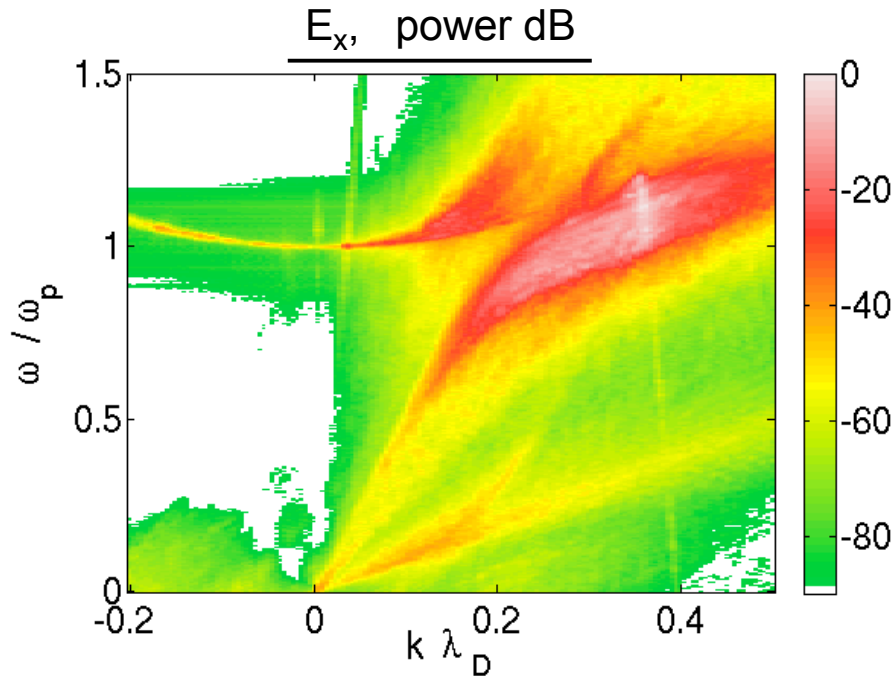
reflected light wave $\Delta\omega/\omega_0=0.0806$



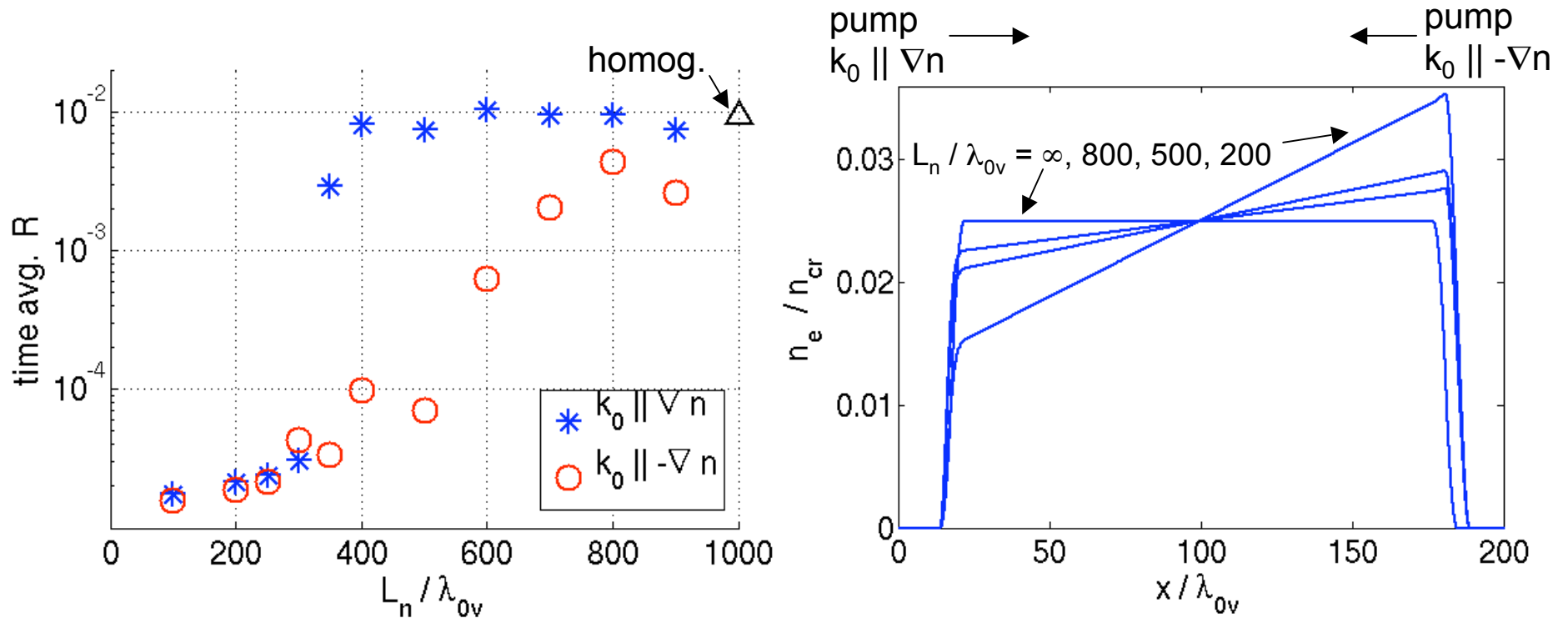


- EAS power level = noise (depends on $\Delta\omega$) + Thomson from laser (indep. of $\Delta\omega$)
- EAS emerges from noise as $\Delta\omega$ decreases. EAS does not amplify seed light-waves, arguing for EATS and against Stimulated Electron Acoustic Scatter (SEAS).

$\Delta\omega/\omega_0 = 0.08$: SRBS downshift, BAMs, and EAWs just as for no bandwidth.



Fixed box size, varying density at endpoints.



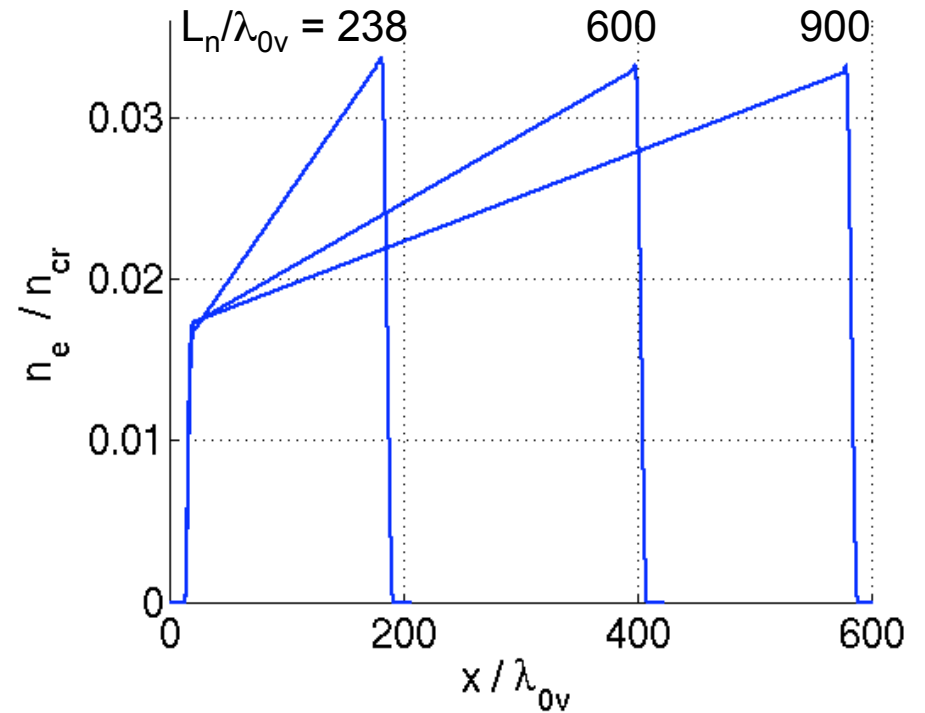
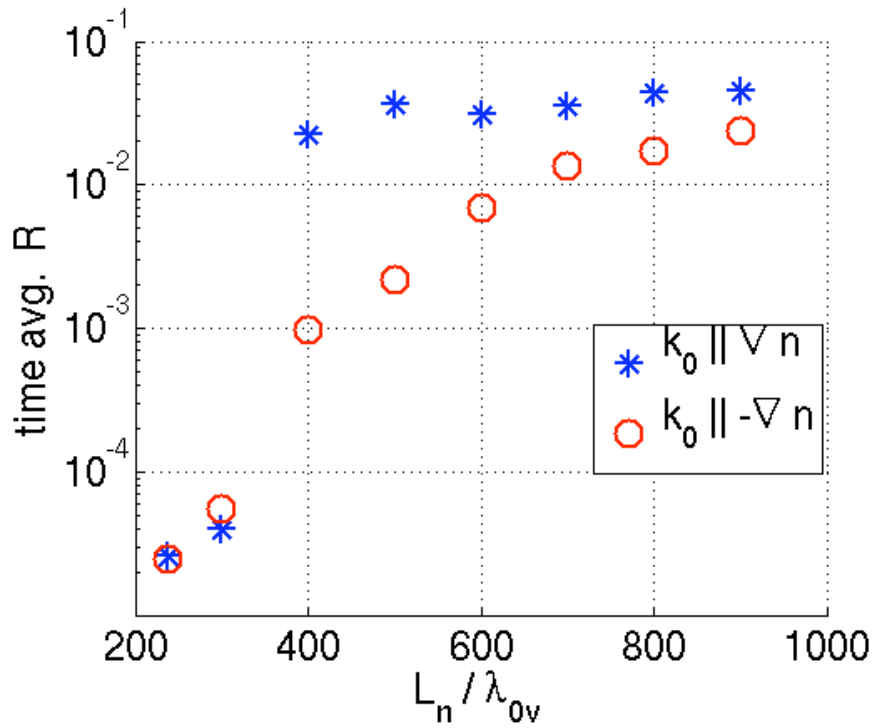
Directional asymmetry: why more reflectivity when pump propagates up the gradient?

R does not increase monotonically with L_n ; perhaps due to regions of higher density (and lower Landau damping) being included for smaller L_n . Interesting to compare to runs with same density range but varying box size...

Inhomogeneity: Similar results for fixed density range but varying box length

$$v_{os}/c = 0.02$$

Fixed density at endpoints, varying box size.



Conclusions

- Beam acoustic decay, electron acoustic Thomson scatter interpretations of electron acoustic scatter supported by spectra, Gauss-Hermite linear modes, bispectral analysis.
- Externally-driven, electrostatic runs reach a steady state, with spatially-varying damping rates and wavenumber shifts reminiscent of Morales-O'Neil. This spatial dependence of the plasma response explains the counter-intuitive increase in plasma-wave amplitude away from the pump entrance in weakly-driven Trident SRBS runs.
- A Krook term can suppress kinetic inflation, even when $\omega_B \sim 6v_K$.
- Broadband seeds do not affect the reflectivity, but EAS vanishes as a distinct peak in the reflected light spectrum as $\Delta\omega$ increases. This shows EAS is not parametrically amplifying seed light waves, but obtains a fixed level due to pump scattering off independently-produced EAWs.
- Inhomogeneous density profiles can prevent SRBS inflation. However, the reflectivity is consistently higher when the pump propagates up (instead of down) the density gradient. Why? Happens if the density endpoints are fixed but the box size is varied, or vice versa.

Comments, questions, reprints? Please leave address
